Protein Science (1997), *6*:1438–1448. Cambridge University Press. Printed in the USA.

The co-crystal structure of unliganded bovine α-thrombin and prethrombin-2: Movement of the Tyr-Pro-Pro-Trp segment and active site residues upon ligand binding

MICHAEL G. MALKOWSKI,[1] PHILIP D. MARTIN, JASON C. GUZIK,[2] AND BRIAN F.P. EDWARDS
Department of Biochemistry and Molecular Biology, Wayne State University, Detroit, Michigan 48201

(RECEIVED December 10, 1996; ACCEPTED April 15, 1997)

Abstract

Unliganded bovine α-thrombin and prethrombin-2 have been co-crystallized, in space group $P2_12_12$, using either ammonium sulfate or polyethylene glycol 2000 (PEG2K), and their structures determined at 2.2 Å and 2.3 Å, respectively. Initial phases were determined by molecular replacement and refined using XPLOR to final R factors of 0.187 (R_{free} = 0.255) and 0.190 (R_{free} = 0.282) for the salt and PEG2K models, respectively. The apo-enzyme form of bovine α-thrombin shows dramatic shifts in placement for the Tyr-Pro-Pro-Trp segment, for Glu-192, and for the catalytic residues His-57 and Ser-195, when compared to 4 thrombin complexes representing different states of catalysis, namely (1) the Michaelis complex (residues 7–19 of fibrinogen Aα with a non-cleavable scissile bond), (2) enzyme-inhibitor complex (D-Phe-Pro-Arg chloromethylketone), (3) enzyme product complex (residues 7–16 of fibrinopeptide A), and (4) the exosite complex (residues 53–64 of hirudin). The structures of bovine and human prethrombin-2 are generally similar to one another (RMS deviation of 0.68 Å) but differ significantly in the Arg-15/Ile-16 cleavage region and in the three activation domains, which are disordered in bovine prethrombin-2, analogous to that seen for trypsinogen.

Keywords: α-thrombin; blood coagulation; prethrombin-2; protein structure; serine proteases; X-ray crystallography

Thrombin (EC 3.4.21.5), a multifunctional serine endoprotease, is generated in the penultimate step of the blood coagulation cascade from the precursor protein prothrombin, and cleaves preferentially after arginine and sometimes lysine. Thrombin is best known as both a major product and a major regulator of the clotting cascade in thrombosis and hemostasis (Fenton, 1988; Davie et al., 1991). Unliganded thrombin is procoagulant and accelerates the clotting cascade through feedback activation of Factors V, VIII, and XI. When complexed with thrombomodulin, thrombin is anticoagulant and activates Protein C, which further inactivates Factors Va and VIIIa. The initial hemostatic plug is generated through the activation of platelets via the binding of thrombin to a specific receptor (Coughlin et al., 1992). Thrombin removes short amino terminal peptides from the Aα and Bβ chains of fibrinogen to generate fibrin polymers and activates factor XIII, which crosslinks the fibrin polymers to stabilize the plug.

In ensuing events, thrombin initiates clot lysis and promotes healing by stimulating the release of tissue plasminogen activator and plasminogen activator inhibitor-1, and the growth of endothelial and smooth muscle cells (Harker & Mann, 1992). Thrombin escalates the inflammatory response by attracting monocytes (Bar-Shavit et al., 1983; Colotta et al., 1994) and by facilitating the migration of leukocytes from blood to tissues through degradation of the constituents of basement membranes (Goldfarb & Liotta, 1986).

Prethrombin-2 is the simplest inactive precursor of α-thrombin and is similar in structure to other zymogens such as chymotrypsinogen and trypsinogen (Vijayalakshmi et al., 1994). Prethrombin-2 is generated from prothrombin through cleavage by Factor Xa in the presence of phospholipid and Ca^{2+} and is ultimately processed into α-thrombin (Rosing & Tans, 1988). The inactive bovine pre-

Reprint requests to: Brian F.P. Edwards, Ph.D., Department of Biochemistry, Wayne State University, 540 E. Canfield Ave., Detroit, Michigan 48201; e-mail: bedward@cms.cc.wayne.edu.

[1]Present address: Department of Biochemistry, Michigan State University, East Lansing, Michigan 48824-1319.

[2]Deceased.

Abbreviations: apoTBN, unliganded bovine α-thrombin; apoTBN/PRE2, crystallographic dimer in asymmetric unit consisting of one molecule of α-thrombin and one molecule of prethrombin-2; ε-thrombin, bovine α-thrombin cut between residues Ala-149A and Asn-149B; PEG, polyethylene glycol; PRE2, prethrombin-2; RMS, root mean square; SDS-PAGE, sodium dodecylsulfate polyacrylamide gel electrophoresis; TBN:Fpa7, bovine thrombin complexed with residues 7f–16f of fibrinopeptide A; TBN:G17ψ, bovine thrombin complexed with residues 7f–19f of the human fibrinogen Aα chain with Gly-17f replaced with pseudo-glycine (–$C(H)_2$–$C(H)_2$–C(O)–); TBN:Hir, human thrombin complexed with residues 53–64 of hirudin; TBN:PPACK, human thrombin covalently inhibited with the inhibitor D-Phe-Pro-Arg chloromethylketone; TBN, α-thrombin; Y60 loop, thrombin residues Tyr-60A, Pro-60B, Pro-60C, Trp-60D, Asp-60E, Lys-60F, Asn-60G, Phe-60H, and Thr-60I; YPPW segment, thrombin residues Tyr-60A, Pro-60B, Pro-60C, and Trp-60D.

cursor, a single chain of 308 residues, becomes the active, disulfide-linked 2 chain serine protease α-thrombin upon cleavage between the Arg-15/Ile-16[3] peptide bond. The larger B-chain has 259 residues and a single glycosylation site (Asn-60G) in both bovine and human α-thrombin. Crystal structures of bovine thrombin complexed with residues 7–16 of fibrinogen Aα (Martin et al., 1992), with a non-cleavable analogue of residues 7–19 of fibrinogen Aα (Martin et al., 1996), with hirudin (Vitali et al., 1992, 1996), and with small molecule inhibitors (Brandstetter et al., 1992) have been determined. Structures have also been determined for similar complexes involving human thrombin (Bode et al., 1989; Grütter et al., 1990; Rydel et al., 1990; Stubbs & Bode, 1992), and the crystal structure of human prethrombin-2 has recently been elucidated (Vijayalakshmi et al., 1994).

Thrombin is more specific than other serine proteases such as trypsin and chymotrypsin, due to two major insertions in the primary structure, the Y60 insertion loop (residues Tyr60A–Thr60I), and the autolysis loop (residues Thr149A–Glu149E) (Fig. 1). The protruding surface loops impose severe steric constraints on potential substrates and inhibitors, such as the Kunitz-type protease inhibitors (Bode et al., 1989, 1992; LeBonniec et al., 1993). The Y60 insertion loop is nine residues longer than the corresponding region in chymotrypsin (Bode et al., 1992). It is highly conserved among 11 thrombin species (Banfield & MacGillivary, 1992), and includes the carbohydrate carrying Asn-60G. Within the loop, residues Tyr-60A and Trp-60D help form the apolar and S2 binding sites respectively (Bode et al., 1989, 1992). The importance of the loop to thrombin's specificity has been shown in the deletion of residues Pro-60B, Pro-60C, and Trp-60D (des-PPW). This mutant leads to an increased accessibility to the active site for bovine pancreatic trypsin inhibitor (BPTI) and to a loss of activity toward fibrinogen, protein C, antithrombin-III, and hirudin without affecting the geometry of the catalytic residues or the structure of the primary specificity pocket (LeBonniec et al., 1993). The autolysis loop is five residues longer compared to chymotrypsin, and shows high variability among known sequenced species (Banfield & MacGillivary, 1992). In most crystal structures of thrombin, the electron density for the autolysis loop is fragmented or absent (Martin et al., 1992; Vitali et al., 1992; Vijayalakshmi et al., 1994; Martin et al., 1996; Vitali et al., 1996).

Further specificity is provided by a strongly basic groove on the surface of thrombin, termed the fibrinogen recognition exosite, that binds macromolecule ligands at acidic residues c-terminal to the scissile bond (Fenton et al., 1988) (Fig. 1). When the exosite is occupied by synthetic peptides corresponding to segments of hirudin, fibrinogen, or heparin co-factor II, an allosteric change occurs within the enzyme's catalytic site that alters the kinetics of hydrolysis for peptide substrates (Dennis et al., 1990; Hortin & Trimpe, 1991; Liu et al., 1991a, 1991b). When thrombin is incubated with hirugen, HPLC, gel filtration, and CD spectral studies indicate thrombin undergoes a conformational change, a change not observed when thrombin is incubated with PPACK (Konno et al., 1988; Mao et al., 1988). Hirudin–thrombin complex formation caused a decrease in the ellipticity of the CD spectrum when compared to the sum of the spectra for free thrombin or hirudin alone, whereas no differences in the spectra were observed for the PPACK–thrombin complex, free PPACK, or free thrombin.

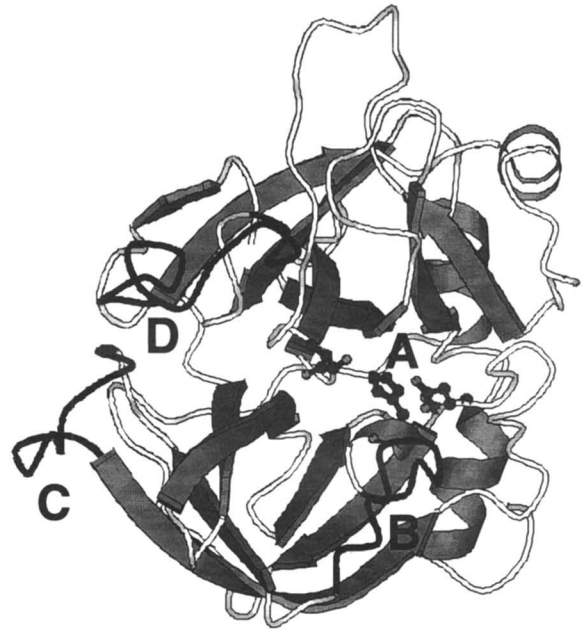

Fig. 1. The thrombin B-chain. A MOLSCRIPT (Kraulis, 1991) rendition of the thrombin B-chain is depicted. Shown in bold are (**A**) ball-and-stick representations of the side chain atoms of catalytic residues His-57, Asp-102, and Ser-195 in the active site cleft, (**B**) the Y60 insertion loop, (**C**) the fibrinogen recognition exosite, and (**D**) the autolysis loop. The A-chain has been omitted for clarity.

A complete picture of these conformational linkages between the active site and the exosite of α-thrombin requires at least three structures—with the active site occupied, the exosite occupied, and neither site occupied. Multiple examples of active site and exosite complexes are available. This paper, which presents the crystal structure of unliganded α-thrombin (apoTBN), co-crystallized by happenstance with one molecule of prethrombin-2, completes the triptych.

Results

The final apoTBN/PRE2 models, crystallized in space group $P2_12_12$ using either polyethylene glycol 2000 (PEG2K) or ammonium sulfate as precipitants, are isomorphous with RMS deviations (RMSDs) on 556 Cα atoms of 0.27 Å. The RMSD between the apoTBN and PRE2 molecules for 233 Cα atoms are 0.38 Å and 0.36 Å, respectively, for the PEG and salt-crystallized structures. The final *R*-factor for apoTBN/PRE2 crystallized from PEG2K is 0.190 (R_{free} = 0.282), while the final *R*-factor for apoTBN/PRE2 crystallized from ammonium sulfate is 0.187 (R_{free} = 0.255) (Table 1). The structures have an estimated mean error in their coordinates of approximately 0.25 Å (Luzzati, 1952) and have excellent stereochemistry when analyzed with the program PROCHECK (Laskowski et al., 1993). On the Ramachandaran plots, all the residues lie within the allowed regions with the exception of residues Glu-1C and Ala-1B (amino terminus of the A chain of α-thrombin) in apoTBN/PRE2 crystallized from PEG2K, and res-

[3]The residue numbers for thrombin in this paper are assigned by homology with chymotrypsin (Bode et al., 1989). Sequential capital letters are used for thrombin residues inserted into the sequence of chymotrypsin, for example, the five residues of the autolysis loop inserted at position 149 (Thr-149A through Glu-149E). Sequence numbers for fibrinopeptide residues and inhibitor residues are distinguished from those for thrombin residues by the suffixes "f" and "i," respectively.

Table 1. *Summary of data collection and reduction*

	apoTBN/PRE2	
Crystallization precipitant	PEG2K	$(NH_4)_2SO_4$
No. of frames	900	830
No. of total reflections	90,801	142,959
No. unique reflections	44,681	47,039
R_{sym},[a] all data ($I > 0\sigma$)	0.072	0.101
Completeness ($F > 2\sigma$)	79%[b]	75%[c]
Completeness, last shell	57%[d]	49%[e]
Space group	$P2_12_12$	$P2_12_12$
a (Å)	87.58	87.52
b (Å)	88.55	87.99
c (Å)	101.03	101.65
No. reflections in refinement[f]	32,058	34,872
No. of atoms	4,636	4,636
No. of water molecules added	205	379
R-factor	0.190	0.187
Free-R factor[g]	0.282	0.255
Mean positional error (Å)[h]	0.27	0.25
RMSD in bond distance (Å)	0.017	0.016
RMSD in bond angle (°)	2.3	2.28
RMSD in improper angle (°)	1.96	1.84
RMSD in dihedral angle (°)	24.7	24.7

[a] R_{sym} is defined as: $\Sigma|I_{hkl} - \langle I\rangle_{hkl}|/\Sigma I_{hkl}$.
[b] Data from 7.0 Å to 2.3 Å resolution.
[c] Data from 7.0 Å to 2.2 Å resolution.
[d] 2.5Å to 2.3Å shell.
[e] 2.4Å to 2.2Å shell.
[f] $F \geq 2\sigma$.
[g] Test set comprised of 10% of the data.
[h] Upper limit (Luzzati, 1952).

idue Thr-147 (autolysis loop) in apoTBN/PRE2 crystallized from ammonium sulfate. The nine other parameters evaluated by PROCHECK are within the bounds established from well-refined structures at equivalent resolution or on the better side of these regions.

By SDS-PAGE analysis, the crystals contain equimolar amounts of prethrombin-2 and α-thrombin (Fig. 2). In both crystal structures, the PRE2 model includes residues 1D through Asp-243 and the α-thrombin model includes A-chain residues 1C through 14L, and B-chain residues 16 through 243. The fibrinogen recognition exosite (72–78), and the autolysis loop (147–151) are disordered in bovine apoTBN and in bovine PRE2. The R15/I16 cleavage region (14L–21) and three activation domains (141–146; 186A–188; 217–224) are ordered in apoTBN but have only fragmented electron density in bovine PRE2 so they were assigned occupancies of 0.01 during refinement of the latter structure. ApoTBN and PRE2 are not compared in detail in this paper because most of the differences involve disordered regions and the changes upon activation are the same as for the human proteins (Vijayalakshmi et al., 1994).

The Na^+ binding site in apoTBN is represented by a water molecule (Wat-1407), which is coordinated to three other water molecules (Wat-1406, Wat-1412, and Wat-1445) and the carbonyl oxygens of Arg-221A and Lys-224. The coordination of Wat-1407 agrees with the coordination of Rb^+ at this site (DiCera et al., 1995) and indicates that the allosteric thrombin molecule in this structure is in its procoagulant or "fast" form (Wells & Dicera, 1992).

Discussion

The crystals of apoTBN/PRE2 were obtained during crystallization trials setup as apo-enzyme controls in our efforts to develop new crystallization conditions for bovine thrombin co-complexes. The mixture of prethrombin-2 and α-thrombin, which has been also observed in experiments to obtain pure prethrombin-2 (Mann, 1976; Vijayalakshmi et al., 1994), occurred here because the prothrombin was not activated completely during the purification of thrombin from bovine plasma. Other thrombin structures crystallized in our laboratory have also been heterogeneous with one molecule of α-thrombin, and one or more molecules of ϵ-thrombin in the asymmetric unit (Martin et al., 1992, 1996; Vitali et al., 1996).

Comparison of bovine and human PRE2

When the complete bovine and human PRE2 models (Vijayalakshmi et al., 1994) are superimposed using ALIGN (Satow et al., 1986), the RMSD for 259 Cα atoms is 0.68 Å. After all the residues with fragmented density that were assigned an occupancy of 0.01 in the refinement are removed, the RMSD for 223 Cα atoms is 0.47 Å, with 21 residues still exhibiting deviations greater than 1.0 Å on Cα positions between bovine and human PRE2. With the exception of Glu-14E through Ile-14K and Asp-189 through Asp-194, these residues are at chain termini or in surface loops that have crystal packing contacts or both.

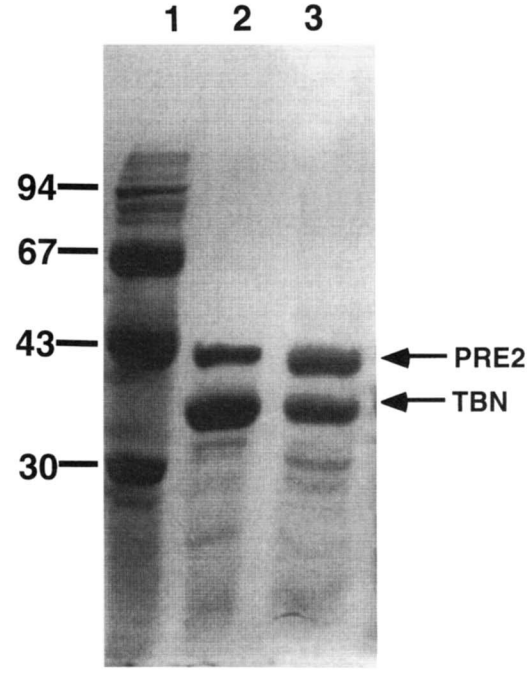

Fig. 2. SDS-PAGE analysis of APO:TBN:PRE2 crystal. A crystal of apoTBN/PRE2 crystallized from PEG2K was washed thoroughly, dissolved in distilled water, and analyzed on a 15% polyacrylamide gel run under reducing conditions. Lane 1 shows low molecular weight standards of 94 kDa, 67 kDa, 43 kDa, and 30 kDa. Lane 2, the starting protein material, and lane 3, the dissolved crystal, show approximately equimolar amounts of prethrombin-2 (M_r = 38 kDa) and α-thrombin (A chain M_r = 5 kDa, B chain M_r = 33 kDa). The bands have anomalously high molecular weights due to the presence of the polysaccharide chain attached to Asn-60G (M_r = 2.5 kDa) in the B-chain.

The autolysis loop, which is disordered in both bovine and human PRE2, is notoriously mobile and not seen in most thrombin structures unless a particular conformation is stabilized by crystal packing contacts (Vijayalakshmi et al., 1994). Similarly, the fibrinogen recognition exosite is empty and disordered in bovine PRE2 but well defined in human PRE2 due to the stabilizing influence of hirugen bound to the exosite.

Activation domains

The electron density for the polypeptide segments corresponding to the Arg-15/Ile-16 cleavage region and the three activation domains is weak in the bovine structure. In human PRE2, these regions have defined density albeit with relatively high-temperature factors. Other zymogen structures show a similar phenomenon for the flexible activation domains. In trypsinogen, the activation domains are disordered even at low temperatures (Bode & Huber, 1978; Singh et al., 1980; Walter et al., 1982), while in chymotrypsinogen, they are well defined but display different conformations in two different crystal forms (Freer et al., 1970; Wang et al., 1985).

Arg-15/Ile-16 cleavage region

The largest differences between the bovine and human PRE2 models are observed for residues 14E through 14K (RMSD = 2.5 Å deviation between seven Cα atoms) in the vicinity of the Arg-15/Ile-16 cleavage region. Bovine PRE2, like bovine and human thrombin, has two α-helical turns in this segment (14D–14G and 14H–14K) whereas human PRE2 has only the first turn (Figs. 3, 4). Bovine and human PRE2 diverge at residue 14H, with human PRE2 becoming more extended through the Arg-15/Ile-16 peptide bond. Bovine PRE2 starts to extend through the Arg-15/Ile-16 bond at Ile-14K, with both structures converging and becoming similar again at Asp-21. The significance of the additional turn of helix in this region is not obvious. The human PRE2 structure was used as the initial model for the refinement of the two PRE2 molecules (ammonium sulfate, PEG2K), and inspection of the "omit" electron density maps clearly showed a different fit for residues 14H through 14K (Figs. 3, 4). However, these residues, in both the bovine and human PRE2 structures, make similar stabilizing interactions with neighboring residues, and are not involved in crystal packing contacts. Moreover, the average B-value for residues 14H through 14K, in bovine and human PRE2, are similar (37.8 Å^2 and 31.5 Å^2, respectively).

Asp-189 through Asp-194 loop

This is the second region in bovine PRE2 that differs significantly from human PRE2. Ala-190 through Gly-193 form a 3_{10}-helical turn in human PRE2, with a stabilizing main chain hydrogen bond between Gly-193 N and Ala-190 O (3.2 Å) (Vijayalakshmi et al., 1994). During the conversion to active enzyme, the movement of this turn to a type II β-bend conformation between Cys-191 and Asp-194 allows for the formation of the Ile-16/Asp-194 ion pair and most of the S1 subsite through the reorientation of the side chain of Glu-192, which becomes solvent exposed (Freer et al., 1970; Vijayalakshmi et al., 1994). Although there is a significant deviation between these loops (RMSD = 0.8 Å for the 6 Cα atoms, maximum deviation = 2.4 Å for Ala-190) in bovine and human PRE2, the 3_{10}-helical turn and hydrogen bond (Gly-193 N ··· Ala-190 O = 3.0 Å) are conserved in bovine PRE2 (Fig. 5). The electron density is slightly fragmented for this stretch of residues in bovine PRE2 and the average temperature factor is 59.7 Å^2, which is more than twice the average temperature factor for the entire structure (26.3 Å^2) and is almost four times higher than the average temperature factor over the same region in the active enzyme (16.1 Å^2). As in chymotrypsinogen and human PRE2, this activation domain is mobile but still structured in bovine PRE2. It becomes stabilized upon conversion to active enzyme, as evidenced by the drop in temperature factors (Freer et al., 1970; Wang et al., 1985; Vijayalakshmi et al., 1994).

Comparison of apoTBN with liganded thrombins

Although the structure of apoTBN is unique among the thrombin structures in the Protein Data Bank in having a disordered exosite, it is otherwise generally similar to that of other well-refined thrombin structures. The exosite is ordered in all other thrombin structures because it is stabilized by a either a ligand such as hirugen (approximately 89%) or crystal contacts or both. The RMSDs on Cα atoms between human TBN:PPACK (Bode et al., 1989), human

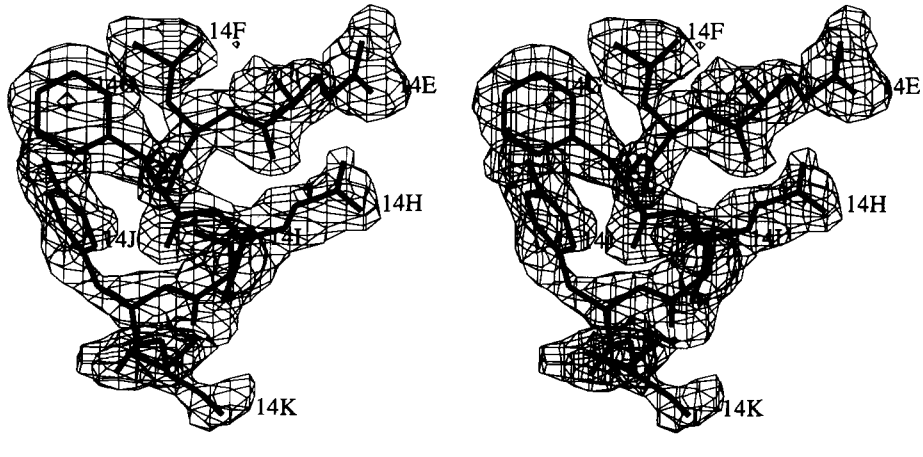

Fig. 3. The electron density for residues 14E through 14K in prethrombin-2. The $2F_o - F_c$ "omit" electron density, contoured at 0.8σ, for residues Glu-14E, Leu-14F, Phe-14G, Glu-14H, Ser-14I, Tyr-14J, and Ile-14K is shown. These residues form two turns of α-helix prior to the Arg-15/Ile-16 cleavage region in bovine prethrombin-2. Residue 14G is a leucine in human prethrombin-2.

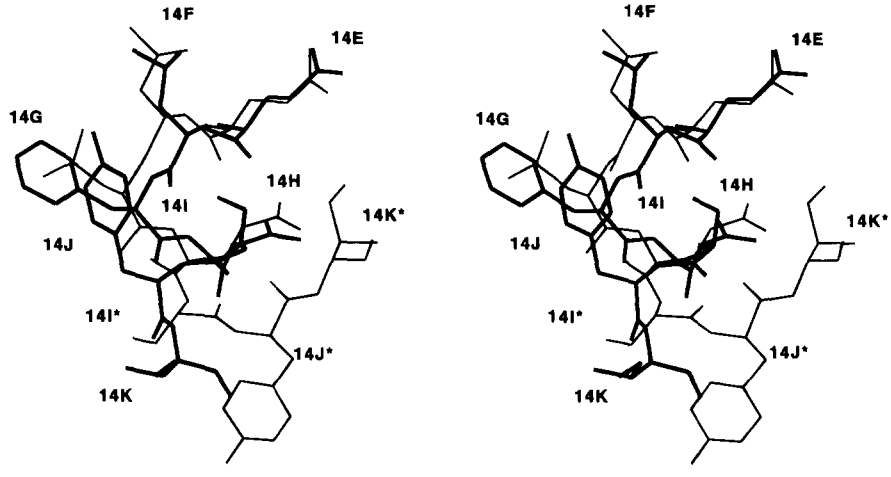

Fig. 4. Comparison of residues 14E through 14K in bovine and human prethrombin-2. Residues 14E through 14K, shown in stereo, in bovine prethrombin-2 (thick lines) form two turns of α-helix before the chain is extended through the Arg-15/Ile-16 cleavage region, whereas the same residues in human prethrombin-2 (thin lines) form only one turn of α-helix. Human prethrombin-2 begins to extend toward the cleavage region at residue 14I (denoted by an *).

TBN:Hir (Vijayalakshmi et al., 1994), bovine TBN:Fpa7 (Martin et al., 1992), and bovine TBN:G17ψ (Martin et al., 1996) are 0.46 Å, 0.41 Å, 0.43 Å, and 0.44 Å, respectively. A total of 20 residues have RMSDs greater than 1.0 Å at their Cα positions. These deviations are reasonable given that the residues lie at the termini of the A or B chain, or contact symmetry-related molecules.

However, residues within the Y60 loop exhibit RMSDs greater than 1.0 Å that do not involve crystal packing contacts. In addition, smaller, yet significant changes are observed for the side chain of Glu-192, versus TBN:Hir, and for the side chains of the catalytic residues His-57 and Ser-195, when compared to both exosite and active site complexes of thrombin.

Glutamic acid 192

The side chain of Glu-192 in apoTBN exists in a different conformation than that seen in TBN:Hir where it is "extended" toward

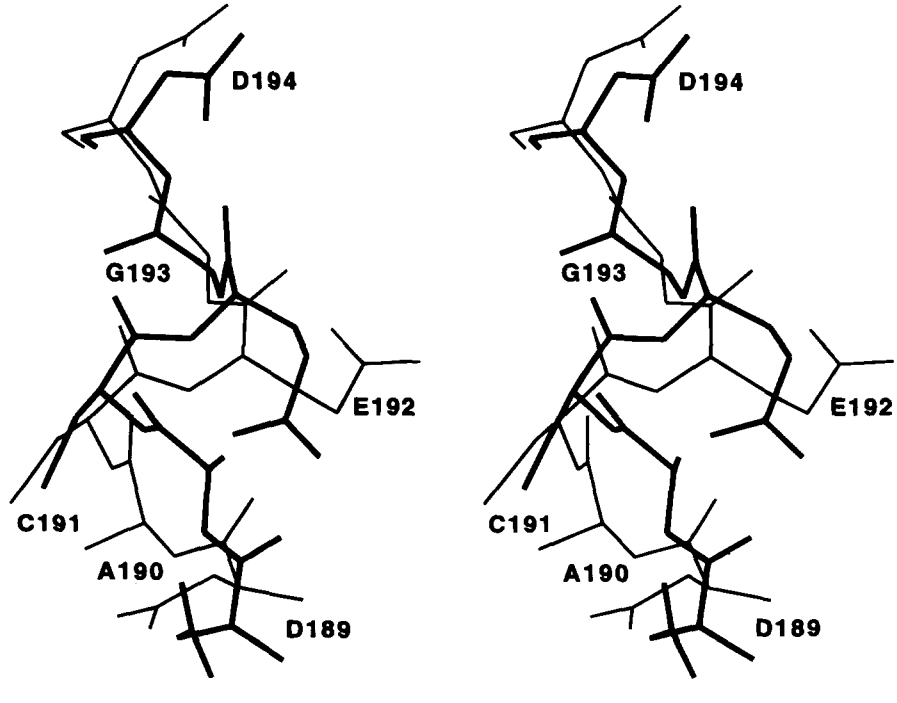

Fig. 5. Comparison of active site residues Asp-189 through Asp-194 in bovine and human prethrombin-2. Bovine prethrombin-2 residues Asp-189, Ala-190, Cys-191, Glu-192, Gly-193, and Asp-194 (thick lines) are superposed upon the same residues in human prethrombin-2 (thin lines) and shown in stereo. These residues lie within an activation domain of prethrombin-2, and although they show a large RMSD between Cα atoms (0.8 Å), their secondary structure is conserved in an analogous manner to that of chymotrypsinogen.

the solvent and TBN:PPACK, where it is bent toward the specificity pocket. The mutation of Glu-192 to Gln, which is the amino acid at this position in trypsin (Vincent & Lazdunski, 1972) and factor Xa (Huang et al., 1993), or to alanine, dramatically enhances the inhibition of thrombin by the Kunitz inhibitors BPTI and TFPI (Guinto et al., 1994), and converts thrombin into an anticoagulant (LeBonniec et al., 1993). In addition, acidic residues, at position P3 in thrombin substrates, are inhibitory due to their proximity to Glu-192 (Erhlich et al., 1990). However, when thrombin is bound at the fibrinogen recognition exosite by something other than fibrinogen (i.e., thrombomodulin or hirugen), it has been shown that the side chain of Glu-192 is converted from a "bent" to an "extended" conformation, thus alleviating negative repulsion between the residues at the binding region and enhancing thrombin's anticoagulant functions (Esmon, 1989; Vijayalakshmi et al., 1994).

In TBN:PPACK, the side chain of Glu-192, is "bent" and points toward the specificity pocket in the vicinity of Arg-3i (Bode et al., 1992). In TBN:G17ψ and TBN:Fpa7, the side chain of Glu-192 is also "bent" but points toward the main chain of Glu-146 and Thr-147, with the Oϵ2 of Glu-192 forming a salt link with the Nη1 of Arg-19f in TBN:G17ψ (Martin et al., 1992, 1996). In apoTBN, the electron density for the side chain atoms Cδ, Oϵ1, and Oϵ2 of Glu-192 are fully defined, whereas the density for Cβ and Cγ is fragmented, an observation noted in other thrombin inhibitor complexes (Vijayalakshmi et al., 1994). Nevertheless, Glu-192 in apoTBN superposes well with the conformations seen in TBN:G17ψ and TBN:Fpa7 with the formation of a hydrogen bond between Oϵ1 of Glu-192 and Nδ2 of Asn-143 (2.6 Å). Therefore, in the unliganded form of α-thrombin, the side chain of Glu-192 appears to take on the "bent" conformation analogous to that seen when substrates and inhibitors bind at the active site (Vijayalakshmi et al., 1994).

Y60 loop movement upon substrate binding

Residues Tyr-60A, Pro-60B, Pro-60C, Trp-60D, Asp-60E, and Lys-60F in bovine apoTBN exhibit the largest deviations on Cα atoms when superimposed with active site and exosite complexes of thrombin. The Y60 loop makes no symmetry-related crystal contacts, and is fully defined by the electron density (Fig. 6). The average temperature factor for residues Tyr-60A, Pro-60B, Pro-60C, and Trp-60D (YPPW segment) in the Y60 loop of bovine apoTBN is 29.5 Å^2. The YPPW segment retains its canonical β-hairpin structure (Bode et al., 1992) but exists in an "open" conformation that exposes the catalytic groove.

When substrate or product is bound in the active site, the YPPW segment moves rigidly like a hydrophobic "lid" to enclose the ligand (Martin et al., 1992; Stubbs & Bode, 1993; Martin et al., 1996). The Cα atoms of Tyr-60A and Trp-60D move 0.9 Å and 2.3 Å, respectively, to the "closed" position in the substrate complex (TBN:G17ψ), and 1.1 Å and 1.8 Å, respectively, in the product complex (TBN:Fpa7) from their "open" positions in apoTBN (Fig. 7). The side chain of Tyr-60A contributes to the formation of the hydrophobic cage (S9 site) surrounding Phe-8f in the fibrinopeptide ligand while the side chain of Trp-60D makes a hydrophobic contact with the side chain of Val-15f in the S2 site (Martin et al., 1992, 1996). No change in the side chain conformations of Tyr-60A or Trp-60D are observed in the substrate or product complexes compared to their conformations in apoTBN (Fig. 7). Therefore, upon substrate binding, the rigid body movement of the YPPW segment makes specific interactions with substrate residues to aid in aligning the scissile bond with respect to the catalytic triad for proper cleavage. In bovine PRE2, where the active site is not fully assembled, the YPPW segment lies between the open and closed positions.

When PPACK, which occupies the S1, S2, and S9 fibrinopeptide subsites on thrombin, is in the active site (TBN:PPACK), the YPPW "lid" also closes over the ligand but the segment moves less—relative to apoTBN—than it does in either the substrate or product complex. Tyr-60A and Trp-60D move 0.57 Å and 1.6 Å, respectively, and in a manner analogous to that seen in TBN:G17ψ and TBN:Fpa7. Tyr-60A packs against Pro2i, which occupies the S2 subsite, while Trp-60D encloses the active site cleft and is exposed to solvent. The YPPW segment in TBN:PPACK is also involved in crystal packing contacts, which possibly limit the movement of the "lid" (Bode et al., 1992).

The position of the YPPW segment in the hirugen exosite complex (TBN:Hir) is similar to that seen in apoTBN. Although the Cα atoms of Trp-60D and Asp-60E move 1.0 Å and 1.1 Å, respectively, relative to apoTBN, the YPPW segment still retains an "open" conformation. The large shift in the Cα positions for Trp-

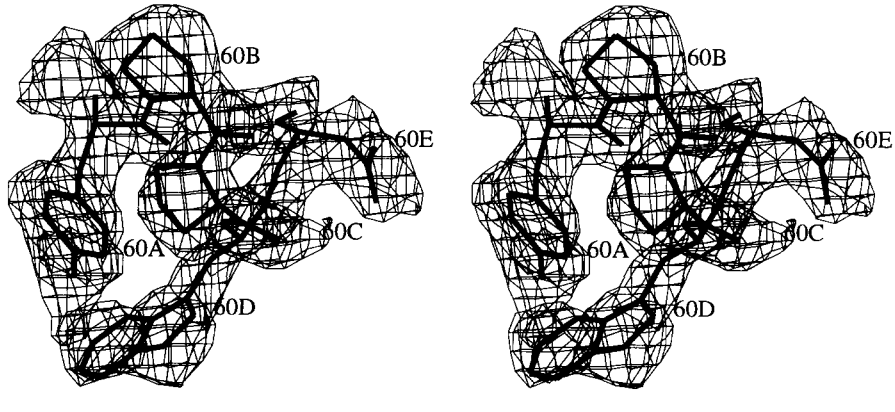

Fig. 6. The electron density for the YPPW loop. The stereo image of the $2F_o - F_c$ "omit" electron density map, contoured at 0.8σ, for residues Tyr-60A, Pro-60B, Pro-60C, and Trp-60D is shown. The loop forms a β-hairpin turn from Tyr-60A that terminates at Asp-60E.

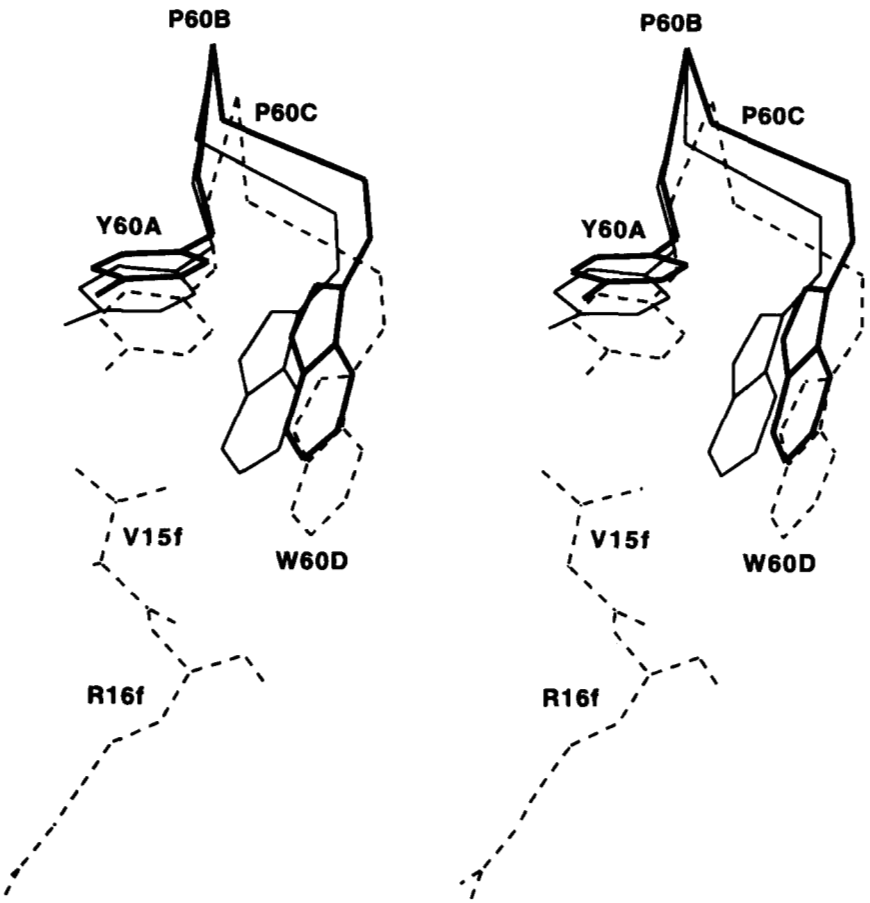

Fig. 7. Movement of the YPPW loop upon substrate binding at the active site. The Cα residues for Tyr-60A through Trp-60D, along with the side chain atoms of Tyr-60A and Trp-60D are shown in stereo for apoTBN (thick lines), TBN:Hir (thin lines), and TBN:G17ψ (complex-III, dashed lines). Substrate residues Val-15f and Arg-16f from TBN:G17ψ (complex-III, dashed lines) are also shown. The YPPW segment moves greater than 1.0Å to stabilize and properly orient the substrate in the active site. The side chains of Pro-60B and Pro-60C have been omitted for clarity.

60D and Asp-60E in TBN:Hir is due to an intermolecular salt link (2.8Å) between Asp-60 Oδ1 in the YPPW segment and Lys-10 Nζ in a symmetry related molecule (Vijayalakshmi et al., 1994).

The polypeptide segment, Tyr-96 through Leu-99, also moves significantly when a substrate or product peptide occupies the active site. These residues form one wall of the hydrophobic pocket with Tyr-96 and Lys-97 positioned adjacent to the YPPW segment at the surface of the molecule. In apoTBN, Trp-96 makes hydrophobic contacts with Pro-60B and Pro-60C when the YPPW segment exists in the "open" position. Upon peptide binding, Trp-96 Cα moves 0.6 Å and Lys-97 Cα moves 0.8 Å in concert with the movement of the YPPW segment (TBN:G17ψ; TBN:Fpa7) (Fig. 8). The movement of Trp-96 maintains the hydrophobic contacts with Pro-60B and Pro-60C that stabilize the YPPW segment and enclose the substrate bound at the active site cleft, while Lys-97 forms a substrate-stabilizing mainchain hydrogen bond between the carbonyl oxygen of Lys-97 and the nitrogen atom of Phe-8f (Martin et al., 1992, 1996). In TBN:PPACK, Trp-96 and Lys-97 also move in unison with the YPPW segment to pack against Pro-60B and Pro-60C.

Catalytic triad

The side chain of the catalytic Ser-195 in apoTBN exhibits a dramatically different conformation to that seen in TBN:G17ψ, TBN:Fpa7, and TBN:Hir (Figs. 8, 9, 10). The polypeptide segment containing Ser-195 is fully defined in electron density (Fig. 9), and the side chain atoms of Ser-195 are equally defined as indicated by the B-values, which are almost twice as low (<17 Å^2) as the average overall B-factor for the entire structure (30 Å^2).

Although the Cα positions within the polypeptide segment containing Ser-195 do not show large deviations among the above structures (less than 0.20 Å), the Ser-195 *Cβ and Oγ positions in* apoTBN differ significantly. An average displacement in the positions, torsion angles, and active site geometry for the side chain atoms of Ser-195 can be calculated from the differences seen in the three independent complexes of TBN:G17ψ and TBN:Fpa7, and in the independent complex of TBN:Hir relative to that seen in apoTBN. Ser-195 in complex-I of TBN:G17ψ and complex-III of TBN:Fpa7 were omitted from comparison because the side chain of Ser-195 exhibits an alternate conformation and forms a hydrogen bond with a backbone carbonyl oxygen (Martin et al., 1992, 1996). The two atoms move 1.2 Å and 0.8 Å, respectively, from their average position in TBN:G17ψ, TBN:Fpa7, and TBN:Hir due primarily to a large change in χ1 from 48.0° in apoTBN to an average of −88.4° ± 11.0° in the complexes.

However, even though there is a large shift in the position of the side chain of Ser-195, the eight hydrogen bonds made by His-57, Asp-102, and Ser-195 to themselves and neighboring residues

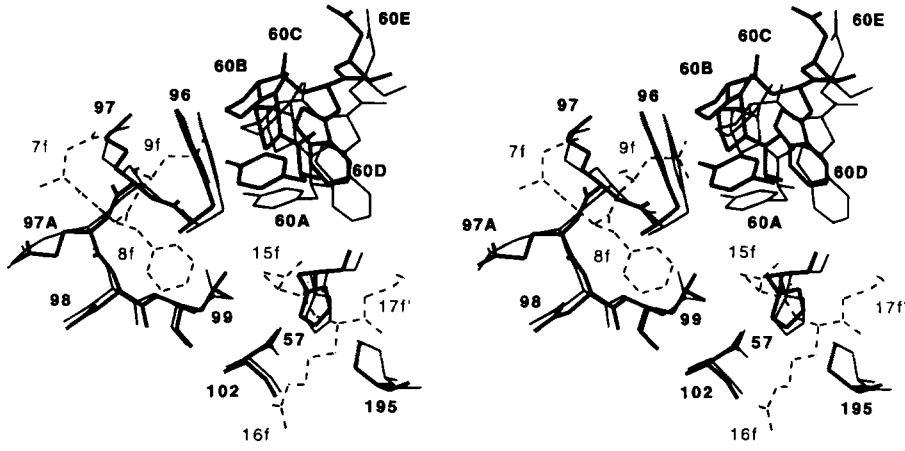

Fig. 8. The movement of Trp-96 and Lys-97 in concert with the YPPW loop. Residues Tyr-60A through Trp-60D, Trp-96 through Leu-99, and active site residues His-57, Asp-102, and Ser-195 are shown in stereo in apoTBN (thick lines) and TBN:G17ψ (thin lines). Substrate residues Asp-7f through Leu-9f in the hydrophobic pocket of thrombin, and Val-15f through "pseudo-glycine" 17f in the active site of thrombin, are also shown (dashed lines). Trp-96 and Lys-97 move in unison with the YPPW loop upon substrate binding. Trp-96 packs against Pro-60B and Pro-60C to stabilize the YPPW loop while Lys-97 forms a substrate-stabilizing main chain hydrogen bond with Phe-8f (Martin et al., 1992, 1996).

in TBN:G17ψ, TBN:Fpa7, and TBN:Hir are maintained within apoTBN. This is accomplished through the compensatory movement of the Nϵ2 atom of His-57 by an average value of 0.5Å, with respect to the position of Nϵ2 in TBN:G17ψ, TBN:Fpa7, and TBN:Hir (Fig. 8, Fig. 10). The conformation seen for the side chain of Ser-195 in apoTBN is not a refinement or fitting artifact. The initial model (TBN:Fpa7) used in molecular replacement calculations and subsequent, independent refinement of the two apoTBN/PRE2 crystal structures (ammonium sulfate, PEG2K), had the "canonical" Ser-195 conformation but rotated spontaneously to the new conformation in both refinements. Moreover, the original conformation was retained in the PRE2 molecule in both refinements.

Theoretical calculations show that nucleophilic attack proceeds optimally when the serine hydroxyl oxygen, carbonyl carbon, and carbonyl oxygen make a right angled triangle that is perpendicular to the plane of the scissile bond (Klebe, 1991). Residues 7f–19f of fibrinogen Aα, with a pseudo-glycine at position 17, bind almost exactly in this fashion in TBN:G17ψ (Martin et al., 1996). When this substrate analog is placed into the active site of apoTBN, the side chain of Ser-195 must rotate 138° about the Cα-Cβ bond to be properly positioned over the carbonyl carbon of the scissile bond (Figs. 8, 10). Specifically, the Cβ–Oγ–$C_{scissile}$ angle differs by 3.4σ in apoTBN (139.5°) compared to the average value of 103.6° ± 10.6° seen in TBN:G17ψ and TBN:Fpa7, and in TBN:Hir when the substrate analog is placed into the active site. Because Ser-195 in TBN:Hir exhibits a similar side chain conformation to that seen in TBN:G17ψ and TBN:Fpa7, substrate binding, at either the fibrinogen recognition exosite, or at the active site of thrombin, causes the side chain of Ser-195 to be reoriented into the proper position for optimal attack of the scissile bond.

Materials and methods

Preparation and analysis of proteins

Bovine α-thrombin was prepared as described previously (Martin et al., 1983) and had between 1500 and 2000 NIH Units per mg of protein. The protein was stored at −80 °C in ammonium phosphate buffer, pH 6.5. SDS-PAGE (Laemmli, 1970) was performed under reducing conditions using 15% pre-formulated gels (Bio-Rad, Hercules, CA).

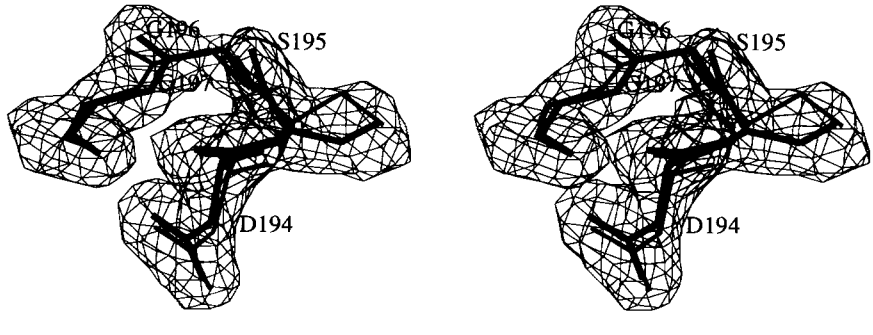

Fig. 9. The electron density for Ser-195 in apoTBN. The $2F_o - F_c$ "omit" electron density, contoured at 0.8σ, for residues Asp-194, Ser-195, Gly-196, and Gly-197 in apoTBN (thick lines), is shown in stereo. Asp-194 through Gly-197 from TBN:G17ψ (thin lines) overlapped onto the apoTBN residues show the disparity in the position of the side chain of Ser-195.

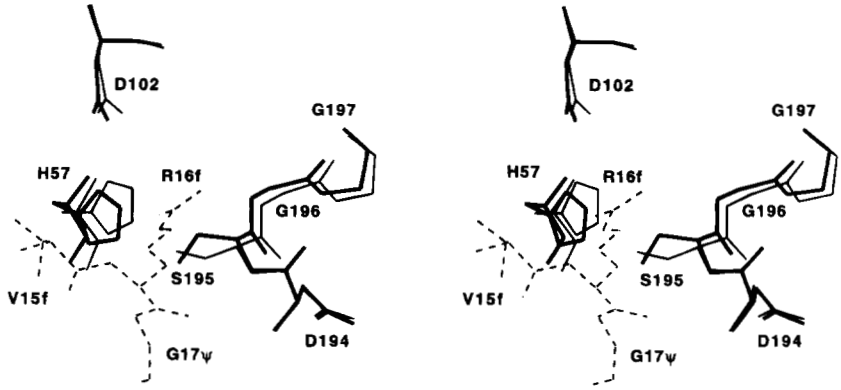

Fig. 10. Movement of His-57 and Ser-195 upon substrate binding. His-57, Asp-102, and residues Asp-194 through Gly-197 in the active site are shown in stereo for apoTBN (thick lines) and TBN:G17ψ (thin lines). Substrate residues Val-15f through "pseudo-glycine" 17f are also shown (dashed lines). The Oγ of Ser-195 must move almost 140° around the Cα–Cβ bond to properly orient itself above the carbonyl carbon of the scissile bond for cleavage. The side chain of His-57 moves in a compensatory fashion to preserve the Nϵ2–Oγ hydrogen bond.

Crystallization

Crystals of apoTBN/PRE2, using polyethylene glycol as the precipitant, were grown by the hanging drop method at 22 °C from a 15 mg/mL protein solution in 50 mM $NaPO_4$, pH 7.3, 100 mM NaCl equilibrated against reservoirs containing 24%PEG2000, 0.1 M NaAcetate, pH 4.6, 0.2 M $(NH_4)_2SO_4$, 0.1% NaN_3. Crystals of apoTBN/PRE2, using ammonium sulfate as the precipitant, were grown in a similar manner, utilizing the hanging drop method at room temperature, from a 7 mg/mL protein solution in 0.25 M $(NH_4)_2PO_4$, pH 6.0 equilibrated against reservoirs containing 38% $(NH_4)_2SO_4$, 0.25M $(NH_4)_2PO_4$, pH 5.8. In addition, the drop solution contained 1% PEG4000. Both crystals are orthorhombic, and contain two, crystallographically independent molecules (apoTBN and PRE2) in the asymmetric unit.

Data collection

Diffraction data were collected at 0 °C, using an XR-85-1 Crystal Cooler (FTS systems, inc., Stone Ridge, NY) on crystals mounted in quartz capillaries using a Siemens X-1000 area detector with a Rigaku RU200H rotating anode X-ray source (40 kV, 70 mA) and a Supper graphite monochromater (CuKα radiation). The data collection was organized using the program ASTRO (Chambers et al., 1992), and were scaled and merged with the program XENGEN (Howard et al., 1987). Details of the data collection and reduction are summarized in Table 1.

Structure solution

Initially, the structure of apoTBN/PRE2 from PEG2K was solved by the molecular replacement method (Rossman & Blow, 1962) using XPLOR (Brünger, 1988) and bovine thrombin from TBN:FpA7 with the fibrinopeptide deleted, as the search model (Martin et al., 1992). The thrombin model was placed in a 120 $Å^3$ P1 orthogonal unit cell with its center of mass at the origin. The cross-rotation function was calculated for the range $\vartheta 1$ = 0–360°, $\vartheta 2$ = 0–90°, and $\vartheta 3$ = 0–180° (Rao et al., 1980) using 4σ data from 7.0 to 4.0 Å resolution. Patterson correlation refinement (Brünger, 1988) of the top 100 solutions identified two rotations, related by 88°, whose coefficients were above 0.90; the next highest rotation had a correlation coefficient of 0.41. The two rotations ($\vartheta 1$ = 104.0°, $\vartheta 2$ = 12.56°, $\vartheta 3$ = 153.46° and $\vartheta 1$ = 98.81°, $\vartheta 2$ = 16.24°, $\vartheta 3$ = 71.18°) were used in translation searches in space group $P2_12_12$. The top peak from each translation search (0.00, 0.240, 0.090, and 0.280, 0.480, 0.080) had correlation coefficients of 0.3434 and 0.2826 that were 4.4σ and 6.3σ greater than the next highest non-solution, respectively. This solution was also used as a starting point for the isomorphous apoTBN/PRE2 structure crystallized from ammonium sulfate.

Inspection of the initial $2F_o - F_c$ electron density maps showed poorly fragmented density for the first five residues at the amino-terminus of the B-chain (I16–S20) and for three other segments (W141–E146, G186A–G188, and E217–K224) in the second molecule of apoTBN/PRE2. The nitrogen atom of Ile-16 forms an ion pair with the carboxylate oxygen of Asp-194 upon activation of prethrombin-2 to thrombin, which is very well defined by electron density in thrombin crystal structures (Bode et al., 1989; Martin et al., 1992, 1996; Vitali et al., 1992, 1996; Vijayalakshmi et al., 1994). The lack of formation of the ion pair and fragmented electron density in this region, as well as for the three other activation domains, led to the hypothesis that the second molecule in each of the crystal structures was prethrombin-2. The presence of prethrombin-2 was verified through SDS-PAGE analysis of the initial protein solution and crystals used during data collection (Fig. 2). At this point, the coordinates for the human prethrombin-2 structure (Vijayalakshmi et al., 1994), with non-identical residues changed to alanine, were placed in the position of the second molecule in the asymmetric unit before proceeding with refinement.

Refinement

The apoTBN/PRE2 data crystallized out of PEG2K were initially refined. The model consisted of one molecule of α-thrombin (A-chain residues Thr-1H through Arg-15; B-chain residues Ile-16 through Ser-247) and one molecule of prethrombin-2 (residues Thr-1H through Glu-247) in the asymmetric unit, with an overall temperature factor of 25 $Å^2$. A "full-refinement" cycle, utilizing the force field parameters developed by Engh and Huber (1991), and consisting of (1) prepstage refinement; (2) simulated annealing utilizing the slow cool annealing protocol with the dynamics temperature starting out at 4000 K and decreasing in intervals of 25 K

to a final temperature of 300 K with 25 steps (0.5 fs/step) of verlet dynamics at each temperature; (3) standard positional minimization; and (4) individual temperature factor refinement, was implemented in XPLOR, and reduced the *R*-factor to 0.252 (R_{free} = 0.344), for 2σ data from 7.0 to 2.3 Å resolution. At this point, computer graphics were used to model the correct side chains for the residues previously changed to alanine that differed between the sequences of bovine and human prethrombin-2, as well as for adjusting poorly fit side chains. Water molecules were then added at positions that were within 2.5–3.5 Å of a hydrogen bond donor or acceptor and had electron density in both $F_o - F_c$ and $2F_o - F_c$ maps.

The initial coordinates of the apoTBN/PRE2 structure from PEG2K were used as the starting point for refinement of the apoTBN/PRE2 structure from ammonium sulfate. Positional and temperature factor refinement dropped the *R*-factor to 0.239 (R_{free} = 0.298) for 2σ data from 7.0 to 2.2 Å resolution. Water molecules were added in an analogous manner to that of the apoTBN/PRE2 structure from PEG.

Structural analysis

The coordinates for the crystal structures of TBN:Hir (entry 1HAH), PRE2 (entry 1HAG), TBN:Fpa7 (entry 1BBR), TBN:G17ψ (entry 1UCY), and TBN:PPACK (entry 1PPB) were obtained from the Protein Data Bank (Bernstein et al., 1977). Hydrogen bonds and torsion angles were calculated using the program QUANTA (MSI/Biosym, Waltham, MA). The criteria for a hydrogen bond are that the three angles C=O···H, O···H–N, and H–N–C be greater than 90° and the distance N···O not exceed 3.3 Å for a "short" hydrogen bond and 4.0 Å for a "long" one (Baker & Hubbard, 1984). Superposition of coordinates between structures was done using the program ALIGN (Satow et al., 1986) and the coordinates for all Cα residues unless stated otherwise. The bovine apoTBN molecule crystallized out of ammonium sulfate was used in the structural comparison with active site occupied bovine thrombin models, which were also crystallized out of ammonium sulfate. Similarly, the bovine PRE2 subunit crystallized out of PEG2K was used in the structural comparison with human PRE2, which was also crystallized out of PEG. Coordinates and structure factors for apoTBN/PRE2 crystallized from PEG2K (accession numbers 1MKW and R1MKWSF) and apoTBN/PRE2 crystallized from ammonium sulfate (accession numbers 1MKX and R1MKXSF) have been deposited in the Protein Data Bank.

Acknowledgments

This work was supported by National Institutes of Health Grant HL57527 (BFPE) and a training fellowship (MGM) from NIH Grant T32 HL07602. This paper is dedicated to the memory of Jason C. Guzik.

References

Baker EN, Hubbard RE. 1984. Hydrogen bonding in globular proteins. *Prog Biophys Mol Biol 44*:97–179.

Banfield DK, MacGillivary RTA. 1992. Partial characterization of vertebrate prothrombin cDNAs: Amplification and sequence analysis of the B chain of thrombin from nine different species. *Proc Natl Acad Sci USA 89*:2779–2783.

Bar-Shavit R, Kahn Z, Fenton JW II, Wilner GD. 1983. Chemotactic response of monocytes to thrombin. *J Cell Biol 96*:282–285.

Bernstein FC, Koetzle TF, Williams GJB, Meyer EFJ, Brice MD, Rodgers JR, Kennard O, Shimanouchi T, Tasumi M. 1977. The protein data bank: A computer-based archival file for macromolecular structures. *J Mol Biol 112*:535–542.

Bode W, Huber R. 1978. Crystal structure analysis and refinement of two variants of trigonal trypsinogen. *FEBS Lett 90*:265–268.

Bode W, Mayr I, Baumann U, Huber R, Stone SR, Hofsteenge J. 1989. The refined 1.9Å crystal structure of human alpha-thrombin: Interactions with D-Phe-Pro-Arg chloromethylketone and significance of the Tyr-Pro-Pro-Trp insertion segment. *EMBO J 8*:3467–3475.

Bode W, Turk D, Karshikov A. 1992. The refined 1.9Å crystal structure of D-Phe-Pro-Arg chloromethylketone-inhibited human α-thrombin: Structure analysis, overall structure, electrostatic properties, detailed active site geometry, and structure function relationships. *Protein Sci 1*:426–471.

Brandstetter H, Turk D, Hoeffken HW, Grosse D, Stürzebecher J, Martin PD, Edwards BFP, Bode W. 1992. Refined 2.3Å X-ray crystal structure of bovine thrombin complexes formed with benzamidine and arginine-based thrombin inhibitors NAPAP, 4-TAPAP, and MQPA. *J Mol Biol 226*:1085–1099.

Brünger AT. 1988. Crystallographic refinement by simulated annealing: Application to a 2.8 Å resolution structure of aspartate aminotransferase. *J Mol Biol 203*:803–816.

Chambers JL, Ortega RB, Campana CF. 1992. Macromolecular data collection strategy. *Am Crystallogr Assoc 50th Ann Meet 20*:87.

Colotta F, Sciacca FL, Sironi M, Luini W, Rabiet MJ, Mantovani A. 1994. Expression of monocyte chemotactic protein-1 by monocytes and endothelial cells exposed to thrombin. *Am J Pathol 144*:975–985.

Coughlin SR, Vu T-KH, Hung DT, Wheaton VI. 1992. Characterization of a functional thrombin receptor: Issues and opportunities. *J Clin Invest 89*:351–355.

Davie EW, Fujikawa K, Kisiel W. 1991. The coagulation cascade: Initiation, maintenance, and regulation. *Biochemistry 30*:10363–10370.

Dennis S, Wallace A, Hofsteenge J, Stone SR. 1990. Use of fragments of hirudin to investigate the thrombin-hirudin interaction. *Eur J Biochem 188*:61–66.

DiCera E, Guinto ER, Vindigni A, Dang QD, Ayala YM, Wuyi M, Tulinsky A. 1995. The Na^+ binding site of thrombin. *J Biol Chem 270*:22089–22092.

Engh RA, Huber R. 1991. Accurate bond angle parameters for x-ray protein structure refinement. *Acta Crystallogr A47*:392–400.

Ehrlich HJ, Grinnell BW, Jaskunas SR, Esmon CT, Yan SB, Bang NU. 1990. Recombinant human protein C derivatives: Altered response to calcium resulting in enhanced activation by thrombin. *EMBO J 9*:2367–2373.

Esmon CT. 1989. The roles of protein C and thrombomodulin in the regulation of blood coagulation. *J Biol Chem 264*:4743–4746.

Fenton JW II. 1988. Regulation of thrombin generation and functions. *Semin Thromb Hemost 14*:234–240.

Fenton JW II, Olson TA, Zabinski MP, Wilner GD. 1988. Anion binding exosite of human α-thrombin and fibrin(ogen) recognition. *Biochemistry 27*:7106–7112.

Freer ST, Kraut J, Robertus JD, Wright HT, Xuong NH. 1970. Chymotrypsinogen: 2.5Å crystal structure, comparison with α-chymotrypsin, and implications for zymogen activation. *Biochemistry 9*:1997–2009.

Goldfarb RH, Liotta LA. 1986. Thrombin cleavage of extracellular matrix proteins: Bioregulatory functions of thrombin. *Ann NY Acad Sci 485*:288–292.

Grütter MG, Priestle JP, Rahuel J, Grossenbacher H, Bode W, Hofsteenge J, Stone SR. 1990. Crystal structure of the thrombin–hirudin complex: A novel mode of serine protease inhibition. *EMBO J 9*:2361–2365.

Guinto ER, Ye J, LeBonniec BF, Esmon CT. 1994. Glu192-Gln substitution in thrombin yields an enzyme that is effectively inhibited by bovine pancreatic trypsin inhibitor and tissue factor pathway inhibitor. *J Biol Chem 269*:18395–18400.

Harker, LA, Mann, KG. 1992. Thrombosis and fibrinolysis. In: Fuster V, Verstraete M, eds. In: *Thrombosis in cardiovascular disorders*. Philadelphia, PA: W.B. Saunders. pp 1–16.

Hortin GL, Trimpe BL. 1991. Allosteric changes in thrombin's activity produced by peptides corresponding to segments of natural inhibitors and substrates. *J Biol Chem 266*:6866–6871.

Howard AJ, Gilliland GL, Finzel BC, Poulos TL, Ohlendorf DH, Salemme FR. 1987. The use of an imaging proportional counter in macromolecular crystallography. *J Appl Crysallogr 20*:383–387.

Huang Z-F, Wun T-C, Broze GJJ. 1993. Kinetics of factor Xa inhibition by tissue factor pathway inhibitor. *J Biol Chem 268*:26950–26955.

Klebe, G. 1991. Correlation of crystal data and charge density with the reactivity and activity of molecules: Towards a description of elementary steps in enzyme reactions. Jeffrey, GA, Pinella, JF, eds. In: *The application of charge density research to chemistry and drug design*. New York: Plenum Press. pp 287–318.

Konno S, Fenton JW II, Villanueva GB. 1988. Analysis of the secondary structure of hirudin and the mechanism of its interaction with thrombin. *Arch Biochem Biophys 267*:158–166.

Kraulis, PJ. 1991. MOLSCRIPT: A program to produce both detailed and schematic plots of protein structures. *J Appl Crystallogr 24*:946–950.

Laemmli, UK. 1970. Cleavage of structural proteins during the assembly of the head of bacteriophage T4. *Nature 227*:680–685.

Laskowski RA, MacArthur MW, Moss DS, Thornton JM. 1993. PROCHECK: A program to check the stereochemical quality of protein structures. *J Appl Crystallogr 26*:283–291.

LeBonniec BF, Guinto ER, MacGillivary RTA, Stone SR, Esmon CT. 1993. The role of thrombin's Tyr-Pro-Pro-Trp motif in the interaction with fibrinogen, thrombomodulin, protein C, antithrombin III, and the kunitz inhibitors. *J Biol Chem 268*:19055–19061.

Liu LW, Vu TKH, Esmon CT, Coughlin SR. 1991a. The region of the thrombin receptor resembling hirudin binds to thrombin and alters enzyme specificity. *J Biol Chem 266*:16977–16980.

Liu LW, Ye J, Johnson AE, Esmon CT. 1991b. Proteolytic formation of either of the two prothrombin activation intermediates results in formation of a hirugen binding site. *J Biol Chem 266*:23632–23636.

Luzzati PV. 1952. Traitement statistique des erreurs dans la determenationdes structures cristallines. *Acta Crystallogr 5*:802–810.

Mann, KG. 1976. Prothrombin. In: Lorand L, ed. *Methods in enzymology, proteolytic enzymes*. New York: Academic Press. pp 123–156.

Mao SJT, Yates MT, Owen TJ, Krstenansky JL. 1988. Interaction of hirudin with thrombin: Identification of a minimal binding domain of hirudin that inhibits clotting activity. *Biochemistry 27*:8170–8173.

Martin PD, Kumar VK, Tsernoglou D, Edwards BFP. 1983. Purification and crystallization of bovine alpha-thrombin, inhibited with PMSF. *Fed Proc 42*:1861–1861.

Martin PD, Robertson WD, Turk D, Huber R, Bode W, Edwards BFP. 1992. The structure of residues 7–16 of the Aα-chain of human fibrinogen bound to bovine thrombin at 2.3 Å resolution. *J Biol Chem 267*:7911–7920.

Martin PD, Malkowski MG, DiMaio J, Konishi Y, Ni F, Edwards BFP. 1996. Bovine thrombin complexed with an uncleavable analog of residues 7–19 of fibrinogen Aα: Geometry of the catalytic triad and interactions of the P1′, P2′, and P3′ substrate residues. *Biochemistry 35*:13030–13039.

Rao SN, Jih JH, Hartsuck JA. 1980. Rotation function space groups. *Acta Crystallogr A36*:878–884.

Rosing J, Tans G. 1988. Meizothrombin, a major product of factor-Xa catalyzed prothrombin activation. *Thromb Haemost 60*:355–360.

Rossman MG, Blow DM. 1962. The detection of sub-units within the crystallographic asymmetric unit. *Acta Crystallogr 15*:24–31.

Rydel TJ, Ravichandran KG, Tulinsky A, Bode W, Huber R, Roitsch C. 1990. The structure of a complex of recombinant hirudin and human α-thrombin. *Science 249*:277–283.

Satow Y, Cohen GH, Padlan EA, Davies DR. 1986. Phosphocholine binding immunoglobulin FAB McPC603: An X-ray diffraction study at 2.7 Å. *J Mol Biol 190*:593–604.

Singh TP, Bode W, Huber R. 1980. Low temperature protein crystallography. Effect on flexibility, temperature factor, mosaic spread, extinction, and diffuse scattering in two examples: Bovine trypsinogen and Fc fragment. *Acta Crystallogr B36*:621–627.

Stubbs MT, Bode W. 1992. The interaction of thrombin with fibrinogen: A structural basis for specificity. *Eur J Biochem 206*:187–195.

Vijayalakshmi J, Padmanabhan KG, Mann KG, Tulinsky A. 1994. The isomorphous structures of prethrombin-2, hirugen-, and PPACK-thrombin: Changes accompanying activation and exosite binding to thrombin. *Protein Sci 3*:2254–2271.

Vincent J-P, Lazdunski M. 1972. Trypsin-pancreatic trypsin inhibitor association. Dynamics of the interaction and role of disulfide bridges. *Biochemistry 11*:2967–2977.

Vitali J, Martin PD, Malkowski MG, Robertson WD, Lazar JB, Winant RC, Johnson PH, Edwards BFP. 1992. The structure of a complex of bovine α-thrombin and recombinant hirudin at 2.8Å resolution. *J Biol Chem 267*:17670–17678.

Vitali J, Martin PD, Malkowski MG, Olsen CM, Johnson PH, Edwards BFP. 1996. Structure of a bovine thrombin–hirudin51–65 complex determined by a combination of molecular replacement and graphics. Incorporation of known structural information in molecular replacement. *Acta Crystallogr D52*:453–464.

Walter J, Steigmann W, Singh TP. 1982. On the disordered activation domain in trypsinogen: Chemical labeling and low temperature crystallography. *Acta Crystallogr B38*:1462–1472.

Wang D, Bode W, Huber R. 1985. Bovine chymotrypsinogen A: X-ray crystal structure analysis and refinement of a new crystal form at 1.8Å resolution. *J Mol Biol 185*:595–624.

Wells CM, DiCera E. 1992. Thrombin is a Na^+ activated enzyme. *Biochemistry 31*:11721–11730.